Article

Dynamic Allosteric Control of Noncovalent DNA Catalysis Reactions

David Yu Zhang, and Erik Winfree

J. Am. Chem. Soc., **2008**, 130 (42), 13921-13926 • DOI: 10.1021/ja803318t • Publication Date (Web): 20 September 2008

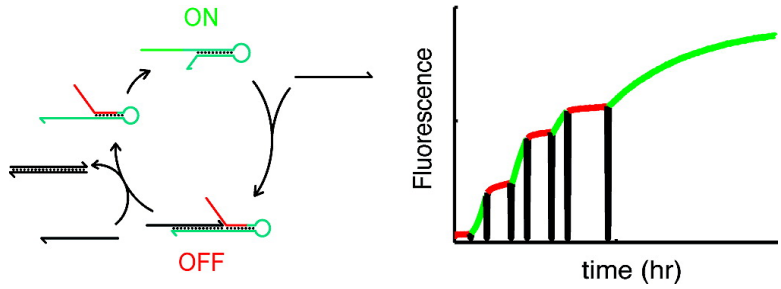

J|A|C|S
ARTICLES

Published on Web 09/20/2008

Dynamic Allosteric Control of Noncovalent DNA Catalysis Reactions

David Yu Zhang* and Erik Winfree

California Institute of Technology, MC 136-93, 1200 East California Boulevard, Pasadena, California 91125

Received May 5, 2008; E-mail: dzhang@dna.caltech.edu

Abstract: Allosteric modulation of catalysis kinetics is prevalent in proteins and has been rationally designed for ribozymes. Here, we present an allosteric DNA molecule that, in its active configuration, catalyzes a noncovalent DNA reaction. The catalytic activity is designed to be modulated by the relative concentrations of two DNA regulator molecules, one an inhibitor and the other an activator. Dynamic control of the catalysis rate is experimentally demonstrated via three cycles of up and down regulation by a factor of over 10. Unlike previous works, both the allosteric receptor and catalytic core are designed, rather than evolved. This allows flexibility in the sequence design and modularity in synthetic network construction.

Introduction

Molecular engineering using only nucleic acids has been demonstrated as a method for constructing aqueous phase logical, structural, mechanical, and catalytic elements.[1−11] Integration of these and other elements will allow the development of complex artificial biomolecular networks that may enable embedded dynamic control of cells, organisms, and synthetic nanomachines.[18] The fine modulation of kinetics is essential for this goal.

In biology, the activities of protein enzymes are finely controlled by the programmed interaction of allosteric ligands that selectively enhance or suppress the protein's catalytic behavior by inducing conformational changes. Recently, unmodified mRNAs have been observed to self-regulate via conformation change upon binding to their metabolite end products.[12−14] In parallel, allosteric ribozymes have been constructed by joining ribozyme sequences with aptamer sequences in vitro.[15−20] The biological relevance of these studies was established with the discovery of similar metabolite-binding RNAs naturally occurring in bacteria.[21] Allosteric ribozymes have also been rationally designed that catalyze other organic reactions.[22]

In the works described above, the allosteric ligands that regulate the catalytic activities are small molecules such as thymine triphosphate (TTP). For the purposes of constructing complex synthetic biochemical networks, many different signal molecules are required for information transmission specificity among simultaneously operating network components. In order for large-scale network construction to be practical, a generalized method for engineering allosteric control elements must be developed, in which the biophysics of molecular interactions can be reliably predicted. Nucleic acids are promising candidates for the role of allosteric regulators because of their high diversity and informational content, as well as their well-understood kinetics and thermodynamics. Accordingly, DNA and RNA have been designed to serve as specific regulators of allosteric ribozymes and deoxyribozymes, culminating in the construction of molecular logic gates[20,23] and translators.[24]

Here, we design and demonstrate an allosteric molecule of DNA that, in its active configuration, can catalyze a noncovalent DNA reaction. Unlike previous work, both the allosteric receptor and the catalytic core are rationally designed, rather than

(1) Zhang, D. Y.; Turberfield, A. J.; Yurke, B.; Winfree, E. *Science* **2007**, *318*, 1121.
(2) Seelig, G.; Yurke, B.; Winfree, E. *J. Am. Chem. Soc.* **2006**, *128*, 12211.
(3) Seelig, G.; Soloveichik, D.; Zhang, D. Y.; Winfree, E. *Science* **2006**, *314*, 1585.
(4) Yurke, B.; Turberfield, A. J.; Mills, A. P.; Simmel, F. C.; Neumann, J. L. *Nature* **2000**, *406*, 605.
(5) Turberfield, A. J.; Mitchell, J. C.; Yurke, B.; Mills, A. P.; Blakey, M. I.; Simmel, F. C. *Phys. Rev. Lett.* **2003**, *90*, 118102.
(6) Winfree, E.; Liu, F.; Wenzler, L. A.; Seeman, N. C. *Nature* **1998**, *394*, 539.
(7) Dirks, R. M.; Pierce, N. A. *Proc. Natl. Acad. Sci.U.S.A.* **2004**, *101*, 15275.
(8) Yin, P.; Choi, H. M. T.; Calvert, C. R.; Pierce, N. A. *Nature* **2008**, *451*, 318.
(9) Yan, H.; Zhang, X.; Shen, Z.; Seeman, N. C. *Nature* **2002**, *415*, 62.
(10) Ding, B.; Seeman, N. C. *Science* **2006**, *314*, 138.
(11) Rothemund, P. *Nature* **2006**, *440*, 297.
(12) Nahvi, A.; Sudarsan, N.; Ebert, M. S.; Zou, X.; Brown, K. L.; Breaker, R. R. *Chem. Biol.* **2002**, *9*, 1043.
(13) Mironov, A. S.; Gusarov, I.; Rafikov, R.; Lopez, L. E.; Shatalin, K.; Kreneva, R. A.; Perumov, D. A.; Nudler, E. *Cell* **2002**, *111*, 747.
(14) Barrick, J. E.; Corbino, K. A.; Winkler, W. C.; Nahvi, A.; Mandal, M.; Collins, J.; Lee, M.; Roth, A.; Sudarsan, N.; Jona, I.; Wickiser, J. K.; Breaker, R. R. *Proc. Natl. Acad. Sci. U.S.A.* **2004**, *101*, 6421.
(15) Tang, J.; Breaker, R. R. *Chem. Biol.* **1997**, *4*, 453.
(16) Schwalbe, H.; Buck, J.; Furtig, B.; Noeske, J.; Wohnert, J. *Angew. Chem. Int. Ed.* **2007**, *46*, 1212.
(17) Ellington, A. D.; Szostak, J. W. *Nature* **1992**, *355*, 850.
(18) Isaacs, F. J.; Dwyer, D. J.; Ding, C. M.; Pervouchine, D. D.; Cantor, C. R.; Collins, J. J. *Nat. Biotechnol.* **2004**, *22*, 841.
(19) Isaacs, F. J.; Dwyer, D. J.; Collins, J. J. *Nat. Biotechnol.* **2006**, *24*, 545.
(20) Penchovsky, R.; Breaker, R. R. *Nat. Biotechnol.* **2005**, *23*, 1424.
(21) Winkler, W.; Nahvi, A.; Breaker, R. R. *Nature* **2002**, *419*, 952.
(22) Amontov, S.; Jaschke, A. *Nucleic Acids Res.* **2006**, *34*, 5032.
(23) Stojanovic, M. N.; Mitchell, T. E.; Stefanovic, D. *J. Am. Chem. Soc.* **2002**, *126*, 3555.
(24) Tabor, J. J.; Levy, M.; Ellington, A. D. *Nucleic Acids Res.* **2006**, *34*, 2166.

Table 1. Domain Sequences

domain	sequence	length (nt)
1	5′-CTTTCCTACA-3′	10
2a	5′-CCTACG-3′	6
2b	5′-TCTCCA-3′	6
2c	5′-ACTAACTTACGG-3′	12
3	5′-CCCT-3′	4
4	5′-CATTCAATACCCTACG-3′	16
4t	5′-CG-3′	2
5	5′-TCTCCA-3′	6
6	5′-CCACATACATCATATT-3′	16
7	5′-TC-3′	2
8	5′-CTTGACTC-3′	8
9	5′-GTATCTAG-3′	8
10	5′-GTCTACTCCTAATG-3′	14

naturally or artificially evolved. The sequences of the DNA molecules involved are shown by domain in Table 1, domains being functional regions of DNA that act as a unit in binding (Figure 1A).

One major advantage of pure DNA constructions is that the patterns of interactions are determined by domain complementarities and secondary structure, and largely independent of the sequences involved except insofar as sequence determines secondary structure.[1−10] For these hybridization-based DNA circuits and reactions, it is expected that designs will function for reasonable choices of sequences for each domain, because their function is based only on the requirement of complementarity between complementary domains. In the sequence design of many simultaneously functioning constructions, it is important to design domains such that nonspecific binding between noncomplementary domains is minimal. This can be done with a number of existing sequence design software packages.[25]

The allosteric catalyst (AC) presented is a single-stranded molecule of DNA that can natively adopt one of two hairpin structures, each with a different stem (Figure 1B).[33] The two states are named AC-ON and AC-OFF to reflect the state's catalytic activity in a downstream reaction. Of the two, AC-ON is the thermodynamically favored state, and AC-OFF quickly rearranges with high probability to form AC-ON.

We demonstrate the AC's catalytic function using the catalyst presented in ref 1 (Figure 1C). In the catalyzed reaction, a single-stranded fuel molecule F reacts with a three-stranded substrate complex S to release a single-stranded output molecule OB and two waste molecules. Domains 4 and 5 on AC must both be single-stranded in order for the catalytic cycle to proceed[1,3,8] and consequently AC-ON is catalytically active and AC-OFF is not. Since AC-ON is the thermodynamically favored state, AC in isolation will be catalytically active.

The catalytic activity of the AC is allosterically regulated by two single-stranded species of DNA, an inhibitor (Inh) and an activator (Act) (Figure 2A). The catalytic activity of AC-ON is suppressed by reaction with Inh: Inh binds to AC via domain $\bar{9}$ and displaces domain 10, causing the resulting Inh:AC complex to adopt AC-OFF's hairpin. With domain 5 and part of domain 4 double-stranded, the Inh:AC complex is catalytically inactive, and thus henceforth referred to as Inh:AC-OFF. The catalytic activity is restored by reaction with Act: Act binds to Inh:AC-OFF via domain $\bar{1}0$, and displaces AC in binding to domains $\bar{9}$ and $\bar{8}$, leaving AC-OFF and duplex waste product Inh:Act. AC-OFF then spontaneously rearranges to the thermodynamically favored AC-ON state. Because Inh and Act are fully complementary strands, they will preferentially bind; in equilibrium, at most one of the two is free in single-stranded form in significant concentration. Introduction of additional Inh or Act into the system (either direct intervention, or production by an upstream reaction) shifts the balance of AC-ON and Inh:AC-OFF and can correspondingly change the rate of catalysis. We

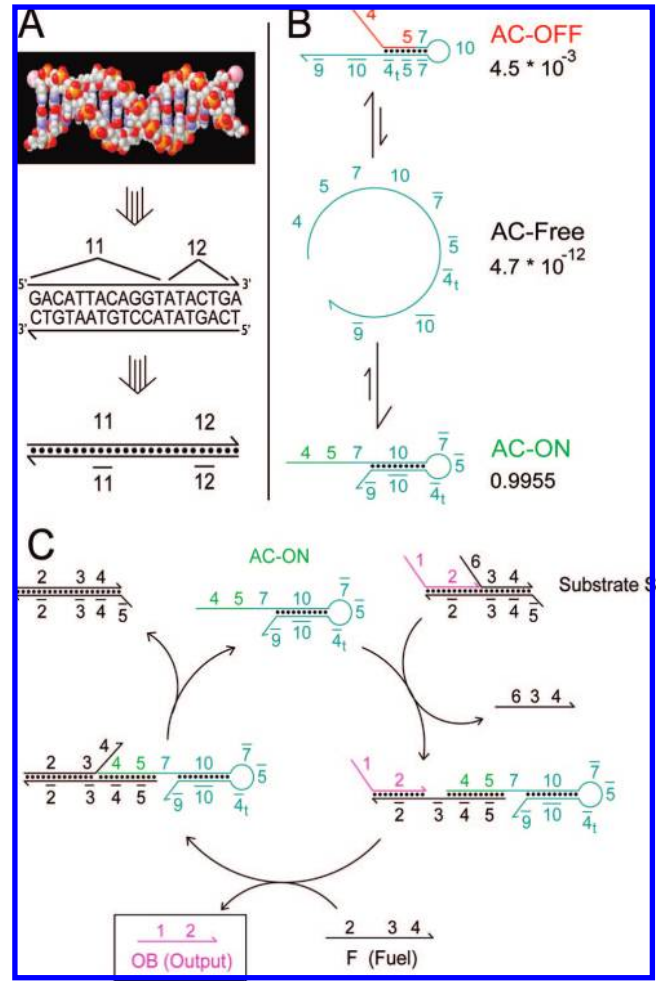

Figure 1. Allosteric DNA hybridization catalyst. (A) DNA abstraction. The double-helix DNA molecule (top) is typically abstracted as two directional lines, one for each strand, with base identities shown (middle). Here, we abstract the DNA molecule one step further by grouping contiguous nucleotides into domains, functional regions of DNA that act as a unit in binding (bottom). Domains are labeled by numbers. Domain $\bar{x}$ is the complement of (and will hybridize to) domain x. The sequences of 11 and 12 are illustrative of the domain concept and not in use for the allosteric catalyst design. (B) The allosteric catalyst (AC). There are three mechanistically important states that the AC can adopt: AC-OFF, AC-free, and AC-ON. Of these three, AC-ON is the most thermodynamically favored (due to the lengths of the hairpin stems; see Table 1), and AC-free is the least thermodynamically favored. The hairpin stem in AC-OFF is designed to be short enough that it can spontaneously open, causing AC to adopt the AC-free state. Then AC will quickly and with high probability fold into AC-ON. The predicted abundances of each state at equilibrium, for the sequences in Table 1, are shown.[26] Domain $\bar{4}t$ is a short two nucleotide domain that is complementary to the 3′-most two nucleotides of domain 4. The presence of domain $\bar{4}t$ helps ensure that the AC-OFF is catalytically inactive. (C) The catalytic cycle. The AC binds to the substrate S via domain 5 and displaces the strand 6·3·4. The newly exposed $\bar{3}$ domain allows the fuel F to bind, displace output OB, and finally displace AC-ON. Domains 4 and 5 on the AC must be single-stranded in order for the catalytic cycle to proceed.

(25) Dirks, R. M.; Lin, M.; Winfree, E.; Pierce, N. A. *Nucleic Acids Res.* **2004**, *32*, 1392.
(26) Zuker, M. *Nucleic Acids Res.* **2003**, *31*, 3406.

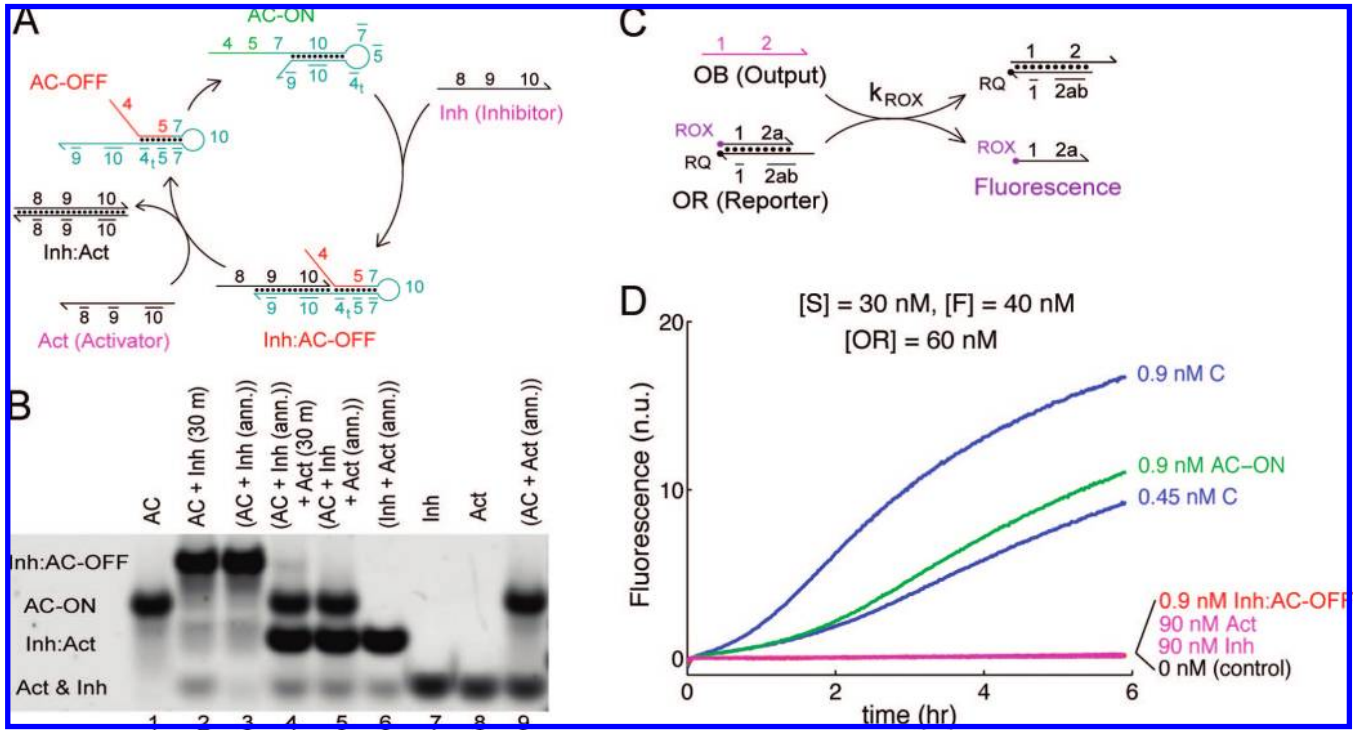

Figure 2. State changing of the AC. (A) State changing by addition of inhibitor (Inh) and activator (Act). Free Inh binds to AC-ON to form the Inh:AC-OFF complex. Free Act binds to Inh:AC-OFF to release AC-OFF and duplex waste product Inh:Act. AC-OFF then spontaneously converts to AC-ON. (B) Analysis by PAGE (12% native gel) of state changing. Here, [AC] = 200 nM, [Inh] = 250 nM, and [Act] = 300 nM. "(ann.)" denotes that species were annealed; "(30 m)" denotes that the reaction proceeded for 30 min. Lanes 1 through 5 show slight smearing because the allosteric catalyst can dynamically switch between its two states over the course of the gel running. (C) The production of OB is quantitated via stoichiometric reaction with reporter complex OR to yield increased fluorescence. ROX denotes the carboxy-X-rhodamine fluorophore (attached to the DNA molecule via an NHS ester), and RQ denotes the Iowa Black Red Quencher. Domain 2 is subdivided into 2a, 2b, and 2c; 2ab consists of 2a and 2b (Table 1). The concentration of the OR reporter complex was always in excess of S to ensure that reporting delay time was approximately consistent. (D) Catalytic activity of the allosteric catalyst. Fluorescence (in all figures) is normalized so that 1 normalized unit (n.u.) of fluorescence corresponds to 1 nM of unquenched fluorophore-labeled strand 1·2a. Various reagents were added at $t \approx 0$. Serving as a control, catalyst C from ref 1 has sequence 4−5. Inh:AC-OFF was prepared by annealing AC with a 3× excess (2.7 nM final concentration) of Inh.

demonstrate dynamic control of production rate of OB with three cycles of up and down regulation.

One desirable feature of the allosteric catalyst design is that Inh and Act are both independent in sequence from the catalytic region and the downstream substrate and fuel. This allows Inh and Act to be designed as products of other reactions with minimal expected cross talk, enabling modular kinetic control of networks.

Materials and Methods

DNA Sequences and Design. Strand design can be done with a number of software packages, and the proposed design should function similarly for many different sequences.[25] The sequences presented here are designed in the following manner, with no claim of being optimized for design or function efficiency. The underlying catalytic substrate and fuel sequences are the same as described in ref 1; only domains 7 through 10 were designed for this work. First, random sequences composed of only A, C, and T were generated for each unbarred domain (i.e., 2). Sequences for the complementary barred domains were constructed accordingly. Next, subsequences expected to be problematic, such as poly-G regions and poly-A regions, were altered by hand. The remaining sequences were then concatenated as appropriate to form the DNA strands (Table 2). These were folded alone and pairwise using the mFold web-server to determine possible cross talk bindings.[26] Some bases at problematic subsequences were then changed by hand to G in the primary domains (and propagated elsewhere as appropriate) to minimize self-folding and pairwise-folding energies. Finally, the strands were checked again on mFold to ensure minimal cross talk.[26]

We chose to do sequence design "by hand" because the sequences involved were so short that this was feasible and possibly faster than specifying the parameters for DNA designs packages. For large-scale circuits, automated design would likely be necessary.

Buffer Conditions. The buffer for all experiments was TE (10 mM Tris·HCl pH balanced to 8.0, 1 mM EDTA), purchased as 100x stock (Sigma-Aldrich), with 12.5 mM $MgCl_2$ added. All experiments and purifications were performed at 25 °C.

Substrate Purification. DNA oligonucleotides used in this study were purchased from Integrated DNA Technologies (IDT), with HPLC purification. Where applicable, fluorophores were attached by IDT as well.

Substrate S and reporter complex OR were further purified by nondenaturing (ND) polyacrylamide gel electrophoresis (PAGE) as follows: strands for each sample were prepared with nominally correct stochiometry at 20 μM and annealed (only nominally correct because it is not possible to quantitate DNA strands with perfect accuracy, so a slight stoichiometric imbalance necessarily exists). A substoichiometric amount (0.2×) of fuel F was added to S, allowing poorly formed substrates to decay into products. The samples were then run on 12% ND PAGE at 180 V for 6 h. The proper bands were cut out and eluted in 2 mL of TE/Mg^{2+} buffer for 2 days. Typical yields ranged from 40% to 60%. Purified complexes were quantitated by measurement of absorbance at 260 nm using an Eppendorf Biophotometer, and concentrations were calculated using extinction coefficients for single- and double-stranded DNA predicted by nearest-neighbor models.[27]

(27) Puglisi, J. D.; Tinoco, I. *Methods Enzymol.* **1989**, *180*, 304.

Table 2. Strand Sequences

strand	domains	sequence
AC	4 5 7 10 $\overline{7}$ $\overline{5}$ $\overline{4}$t $\overline{10}$ $\overline{9}$	CATTCAATACCCTACG TCTCCA TC GTCTACTCCTAATG GA TGGAGA CG CATTAGGAGTAGAC CTAGATAC
Inh	8 9 10	CTTGACTC GTATCTAG GTCTACTCCTAATG
Act	$\overline{10}$ $\overline{9}$ $\overline{8}$	CATTAGGAGTAGAC CTAGATAC GAGTCAAG
F	2 3 4	CCTACGTCTCCAACTAACTTACGG CCCT CATTCAATACCCTACG
OB	1 2	CTTTCCTACA CCTACGTCTCCAACTAACTTACGG
SB (part of S)	6 3 4	CCACATACATCATATT CCCT CATTCAATACCCTACG
LB (part of S)	$\overline{5}$ $\overline{4}$ $\overline{3}$ $\overline{2}$	TGGAGA CGTAGGGTATTGAATG AGGG CCGTAAGTTAGTTGGAGACGTAGG
OF (part of OR)	1 2a	CTTTCCTACA CCTACG
OQ (part of OR)	$\overline{2}$b $\overline{2}$a $\overline{1}$	TGGAGA CGTAGG TGTAGGAAAG

Annealing. All annealing processes were performed with an Eppendorf Mastercycler Gradient thermocycler. The samples were brought down from 95 to 20 °C at a constant rate over the course of 90 min.

Gel Electrophoresis. ND PAGE was run on 12% acrylamide (19:1 acrylamide:bis), diluted from 40% acrylamide stock (Ambion). ND loading dye containing Xylene Cyanol FF (XCFF) in 50% glycerol was added to all samples, achieving final gycerol concentration of 10% by volume. Gels were run at 25 °C using a Novex chamber with external temperature bath. Gels were stained with Sybr-Gold stain (Invitrogen), and scanned with a Bio-Rad Molecular Imager. The formation gel shown in Figure 2B was run at 120 V for 1 h.

Spectrofluorimetry Studies. Spectrofluorimetry studies were done using a SPEX Fluorolog-3 (Horiba) with 1.6 mL 119-004F synthetic quartz cells (Hellma). The excitation was at 588 nm, while emission was at 602 nm (optimal signal for ROX fluorophore). Slit sizes used are 2 nm for both excitation and emission monochromators for net reaction studies. Experiments shown in Figures 2D and 3A were done with integration time of 10 s for every 60 s time point. The experiment shown in Figure 3C was done with integration time of 1 min for every 5 min time point.

Prior to each experiment, all cuvettes were cleaned thoroughly: each cuvette was washed 15 times in distilled water, once in 70% ethanol, another 5 times in distilled water, and finally once more in 70% ethanol.

Experiments start with 1.5 mL of initial solution, and up to 51 μL of high concentration stock was added at later time points as indicated. Fluorescence values were adjusted for dilution as calculated by volume changes. The reported concentrations of species decrease 4% over the course of the experiments due to dilution. For the slit size, concentrations, and times chosen, no measurable photobleaching was observed.

Fluorescence Normalization. Fluorescence (in all figures) is normalized so that 1 unit of fluorescence corresponds to 1 nM of unquenched fluorophores (Figure 2D). This normalization is based on the fluorescence levels of two annealed samples: a negative control with no substrate S and a positive control with 30 nM S. In both samples, [F] = 40 nM and [OR] = 60 nM.

Carrier Strands. It has been observed that DNA sticks nonspecifically to pipet tips, so that serial dilutions lead to stocks more dilute than expected.[1] Unfortunately, this loss is not consistent, so we could not compensate for tip loss with additional reagent. Instead, we introduced into all dilute stocks (1 μM and below) a nonreactive 20 nt poly-T "carrier" strand, at a concentration of 1 μM. Because pipet tip loss is nonspecific, the majority of DNA loss would be of the carrier strand, and serially diluted stocks are only slightly more dilute than expected. Poly-T strands have minimal influence the reactions of other DNA molecules.[1]

Results and Discussion

State Changing. The use of partially complementary nucleic acid molecules as regulators to effect state changes has been demonstrated for RNA switches,[18,19] DNA motors,[4,32] and DNA catalysts.[1,5,7] Their kinetics are generally rate limited by the second-order initiation reaction, which can be adjusted based on the lengths and sequences of of the nucleic acids involved. In the limit of long single-stranded domains, these rates approach the hybridization rate of cDNA strands.

Although it is desirable for the kinetics of state switching to be as fast as possible, the rate constants need not be quite as high as those of the underlying catalytic mechanism, because high concentrations of regulators Inh and Act can be used to induce a higher rate. The efficacy of state-switching by Inh and Act is demonstrated by ND PAGE in Figure 2B. In isolation, AC forms a well-defined band, indicating the predominance of AC-ON over AC-OFF. Upon addition of slight excess (1.25×) of Inh, almost all of AC migrates in the Inh:AC-OFF band after 30 min of reaction, indicating that reactions are fast on this time scale. Similarly, addition of a slight excess (1.5×) of Act displaces almost all of Inh from Inh:AC-OFF within 30 min, forming the duplex band Inh:Act and regenerating the AC-ON band.

The time scale of the rearrangement from AC-OFF to AC-ON can be estimated from DNA thermodynamics and known rate constants: the rate at which AC-OFF opens to form AC-Free should be similar to the rate at which two complementary strands with similar binding energy dissociate. This is calculated to be $k_f\, e^{-\Delta G^o/RT}$, where k_f is the rate constant of DNA hybridization and ΔG^o is the energy of binding. Recent reported measurements of this value range from 10^5 to 10^6/M/s.[28] However, our own experiments in TE/Mg^{2+} buffer with DNA molecules of similar nucleotide compositions in similar buffer conditions suggest a hybridization rate of $k_f = 3 \times 10^6$/M/s (data not shown). Using the latter value and AC-OFF's free energy (−12.3 kcal/mol, as predicted by mFold), the opening rate is estimated to be 3×10^{-3}/s, giving a time scale of about 5 min. Using lower values of k_f, the opening rate is accordingly decreased.

The unstructured AC-Free state then very quickly adopts either the AC-ON or the AC-OFF fold. Since there are more bases in the stem of AC-ON than in AC-OFF, AC-Free is more likely to fold into AC-ON. This implies that the expected time for rearrangement is no more than 10 min. In contrast, similar arguments predict that AC-ON (−15.5 kcal/mol) opens to the AC-Free state on a time scale of about 18 h.

Catalytic Activity of the Allosteric Catalyst. The catalytic activity of AC in its various states is inferred by production of the output molecule OB. This is measured using a fluorescent

(28) Gao, Y.; Wolf, L. K.; Georgiadis, R. M. *Nucleic Acids Res.* **2006**, *34*, 3370.

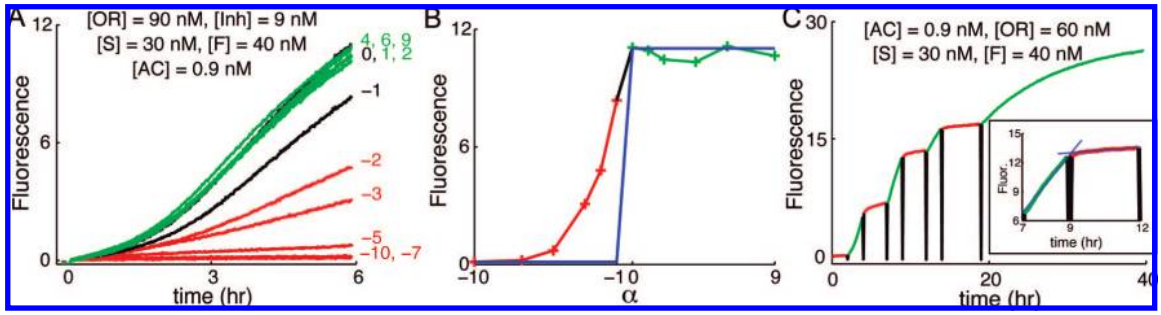

Figure 3. Allosteric catalyst behavior. (A) Dependence of catalytic behavior on the balance of [Act] and [Inh]. [S] = 30 nM = 1x, [F] = 40 nM = 1.3x, [AC] = 0.9 nM, [Inh] = 9 nM. Various amounts of Act were added at $t = 0$ min, with the number label shown being the value of α, the stoichiometric excess of Act. Red shows where the AC is expected to be OFF (Inh:AC-OFF); green shows where AC is expected to be ON (AC-ON). (B) Sigmoidal activation curve. The total catalytic activity over 6 h (from (A)) is plotted against α. Blue trace denotes the expected behavior when AC, Inh, and Act are in equilibrium. (C) Dynamic switching. Initially, 0.9 nM AC is annealed with 2.7 nM Inh. Reagents were added to cause concentration changes as follows: 20 nM Act at $t = 2$ h, 40 nM Inh at $t = 4$ h, 60 nM Act at $t = 7$ h, 80 nM Inh at $t = 9$ h, 100 nM Act at $t = 12$ h, 120 nM Inh at $t = 14$ h, 140 nM Act at $t = 19$ h. The fluorescence level was adjusted for dilution by multiplying by the dilution factor where appropriate. (C, inset) Rate fitting for observed activity between 7 and 12 h. The production rate of OB was fit to be 3:0 nM/h for AC-ON, and 0:18 nM/h for Inh:AC-OFF (blue traces).

reporter complex OR: OB reacts stochiometrically with OR to release an unquenched fluorescent strand (Figure 2C). Before OB is released from the catalytic substrate S, it does not react with OR.

Figure 2D shows the catalytic turnover of AC-ON, Inh:AC-OFF, and control catalyst C. The suppression of catalysis in Inh:AC-OFF is almost complete; the fluorescence levels of the reaction with 0.9 nM Inh:AC-OFF is indistinguishable from that of the control experiment with neither C nor AC. On the other hand, AC-ON retains catalytic activity: 0.9 nM catalyze the release of over 10 nM of OB over 6 h. This represents a 40% slowdown compared to control catalyst C, which is signficant but not critical. The slowdown is suspected to be due to steric hindrance and/or electrostatic repulsion: domain 9 is close to the active catalytic domains 4 and 5 and may interfere with the binding of those domains to substrate S.

Inh and Act are both independent in sequence from the catalytic region and the downstream substrate and fuel, and thus are expected not to show any catalytic activity at all. This is indeed the case, as even 90 nM of Act or Inh alone failed to cause any observable reaction.

Activation of Catalytic Activity. The catalytic activity of the AC changes according to the balance of Inh and Act. Define α to be the stochiometric excess of Act over Inh relative to AC: $\alpha = ([\text{Act}]_{\text{total}} - [\text{Inh}]_{\text{total}})/[\text{AC}]_{\text{total}}$. When AC and its allosteric effectors are at equilibrium, the catalytic activity can be divided into three regimes based on the value of α. For $\alpha \leq -1$, nearly every molecule of AC is expected to be bound in the Inh:AC-OFF state, and catalytic activity should be minimized. For $-1 < \alpha < 0$, some but not all molecules of AC are bound in Inh:AC-OFF, and the catalytic activity is at an intermediate value depending on the exact value of α. For $\alpha \geq 0$, nearly every molecule of AC is free in the AC-ON state, and the catalytic activity should be maximized (Figure 3B).

When the AC is used as part of a larger dynamic network, equilibrium is not maintained during function. To characterize the dynamic behavior of AC's activation, we preannealed the AC with a 10× excess of Inh, and then added various amounts of Act (Figure 3A). The net effect over 6 h of reaction is summarized in Figure 3B.

The major difference between these experiments and the cases when Inh is preannealed with Act is that the AC shows partial catalytic activity when $\alpha < -1$. In constrast, when $\alpha > 0$, the catalytic activity is very close to that of AC-ON. The latter

Table 3. Catalytic Activity Based on State

time (h)	state	OB production rate (nM/h)
0–2	OFF	0.00
2–4	ON	3.5
4–7	OFF	0.24
7–9	ON	3.0
9–12	OFF	0.18
12–14	ON	1.6
14–19	OFF	0.08

suggests that switching from Inh:AC-OFF to AC-ON is relatively fast, while the former suggests that the reverse process is relatively slow: when $\alpha < -1$, the amount of Act added is lower than the amount of free Inh, but nonetheless some Act will react with Inh:AC-OFF rather than free Inh. The resulting AC-OFF rearranges quickly into the active AC-ON state, remaining in solution until it reacts once again with free Inh. This last step being slow on the time scale of the experiment explains the continued catalytic activity for $\alpha < -1$.

The relatively slower kinetics of turning the AC off with Inh is suspected to be due to nonspecific binding interactions between the $\bar{9}$ domain and the 4, 5, and 7 domains. The close proximity between these domains means that the local concentrations are very high, so that one- and two-base pairings, which normally do not form, may exist fleetingly. Inaccessibility of the $\bar{9}$ domain is expected to decrease the rate of state changing, because the binding of Inh to AC-ON is initiated and rate limited by the binding of Inh's 9 domain to AC-ON's $\bar{9}$ domain. In constrast, Inh:AC-OFF does not have a 3′ overhang that nonspecifically interacts with Inh's 8 domain, so the rate of switching from Inh:AC-OFF to AC-ON is not reduced.

Dynamic Switching. The AC can be dynamically switched between its catalytically active (AC-ON) and inactive (Inh:AC-OFF) states. Figure 3C shows the production of OB as modulated by addition of Inh or Act at various time points (shown by black spikes). There is a clear difference in the slopes between when Act was in excess (shown in green) and when Inh was in excess (shown in red).

The rates of production of OB between reagent additions are fitted (Figure 3C, inset), and the results are summarized in Table 3. The first 20 min of data after reagent additions were not used for these fits. The decrease in production rate of OB over time can be attributed to decreasing substrate (S) and fuel (*F*)

concentrations, and to a lesser extent accumulated DNA loss to pipet tips (see Materials and Methods, subsection Carrier Strands).

The kinetics of switching AC-ON to Inh:AC-OFF is seen to be significantly slower than that of the reverse (time scale of approximately 30 min, as opposed to less than 5 min), supporting the hypothesis that switching the AC off is significantly slower than switching it on. Given the excess concentrations of Inh and Act at various times, we estimate the second order reaction rate between AC-ON and Inh to be roughly 3×10^4/M/s, and that between Inh:AC-OFF and Act to be greater than 2×10^5/M/s.

Conclusions

We have demonstrated allosteric control of noncovalent DNA-based catalysis based on alternative hairpin folds. Two molecules controlled the catalytic activity, a noncompetitive inhibitor, and an activator that competitively inhibits the inhibitor. The activator and inhibitor have the same form (single-stranded DNA molecules of similar size) as the released product molecule of the catalytic reaction. Thus, they can be the products of other synthetic biomolecular reactions, released dynamically through the course of operation.

The hybridization-based mechanism by which the allosteric catalyst changes physical and catalytic states is simple and well understood.[32] This method of state control can, in principle, be extended to apply to other nucleic acid based constructions, such as catalytic networks, logic gates, structural assembly, etc.

The preferential binding of the inhibitor Inh to activator Act causes a sigmoidal nonlinearity between catalytic activity and the amount of activator added, given a constant inhibitor concentration (Figure 3B). Similar mechanisms have been biologically observed in kinase cascades to produce ultrasensitivity, filtering out biochemical "noise".[31] From the network construction point of view, it has been proposed that such thresholding behavior can be used to convert between analog and digital representations of information in chemical reaction networks.[29] Recently, thresholds constructed from the competitive binding of mRNA and DNA have been used to build bistable transcriptional networks.[30] Thus, the current work may be used to engineer enzyme-free reaction networks robust to noise.

In previous work on allosteric ribozymes and riboswitches, the identities of the allosteric effectors were determined by aptamer sequences involved and cannot be easily modified. In this work, the allosteric effectors are molecules of DNA whose sequences can be easily programmed: they are independent of the catalytic core, as well as independent of the output molecule. Thus, many different allosteric effectors should be able function simultaneously without significant cross talk.

Acknowledgment. The authors were supported by NSF grants 062254 and 0728703 to E.W. D.Y.Z. is supported by the Fannie and John Hertz Foundation.

JA803318T

(29) Magnasco, M. O. *Phys. Rev. Lett.* **1997**, *78*, 1190.
(30) Kim, J.; White, K. S.; Winfree, E. *Mol. Syst. Biol.* **2006**, *2*, 68.
(31) Ferrell, J. E. *Trends Biochem. Sci.* **1996**, *21*, 460.
(32) Yurke, B.; Mills, A. P. *Genetic Programming Evolvable Machines* **2003**, *4*, 111.
(33) The design of the AC must consider the possibility of pseudoknot formation due to necessary sequence self-complementarity. For the presented design, the hairpin stem regions are short enough that we do not expect significant pseudoknot formation.